111

MULTIPLE INPUT DESCRIBING FUNCTION FOR NON-LINEAR ANALYSIS OF GROUND AND AIR RESONANCE

Vincenzo Muscarello, Giuseppe Quaranta

Dipartimento di Ingegneria Aerospaziale, Politecnico di Milano
{muscarello,quaranta}@aero.polimi.it

Abstract

Aeroelastic stability is a key issue that drives the design of modern rotorcraft. The robustness of stability analysis is fundamental to determine the amount of freedom a designer has in defining the key properties in specific rotorcraft problems dominated by stability. The paper presents an effective technique to investigate the effect of nonlinearities on the ground resonance stability, resorting to the multi input describing function. In this way it is possible to investigate the cases when multiple harmonics are injected into a nonlinear component, a typical condition for rotorcraft components. To show the potential of the method, an application that considers a nonlinear model for hydraulic lead-lag dampers is presented.

1 INTRODUCTION

Helicopter rotors are subject to potentially destructive instabilities due to the interactions between the main rotor dynamics and its flexible support, usually denominated ground resonance. The basics of the phenomenon are well known and understood, see [2, 9]. It involves the coupling of the naturally lightly damped blade inplane motion with the underlying airframe elastic motion. This problem usually affects helicopters that mount an articulated rotor when on the ground, sitting on the landing gear, whereas soft-in-plane hingeless rotors may experience the similar problem known as air resonance in flight [3]. To solve the problem, lead-lag damping needs to be added on rotor blades, either using hydraulic dampers or simpler, and more reliable, elastomeric elements. In any case the sizing of this element is always the result of a trade-off study to harmonize the requirement of high damping for stability with the need to reduce the loads transmitted to the hub by the blades.

Linear analysis methods are able to predict the critical stability boundaries, and so they can be used to design the lag dampers that must be applied to rotor blades. To cope with the significant uncertainty in the physical characterization of these components, it is possible to tackle the problem by means of the Robust Control Theory framework as shown in [11].

However, modern helicopters rarely exhibit destructive resonances, but they may be subject to limit cycle oscillations (LCO), see [18, 19, 15, 4]. In order to predict these LCO conditions it is necessary to consider the contribution of nonlinearities. The identification of LCO conditions can be performed by using the Describing Function approach presented in Ref. [10], which allows to keep into account multiple nonlinearities in the same model. The method of Ref. [10] is here extended to cope with the peculiar aspects required when the model of the system includes at the same time a component in a fixed reference frame, the airframe, and a set of rotating bodies such as the blades. It will be shown that this leads naturally to the necessity to consider Multiple Input DF (MIDF) approaches. In fact, if the starting hypothesis says that the response of the flexible support is dominated by a single harmonic ω, it is possible to show that the lead-lag dampers mounted on rotor blades, so in the rotating reference frame, are in general excited by two harmonics, the regressive $\omega - \Omega$ and the progressive $\omega + \Omega$, where Ω is the angular velocity of the rotor. The application of the DF approach to the ground resonance problem is not new (see Refs. [19, 7]), however here for the first time the problem is approached using the MIDF that allows to address also the problem of LCO that arise when cyclic commands are applied to the rotor, a case where a the multi-frequency nature of the damper input signal can not be neglected.

In this paper the investigation will be concentrated on the lead-lag dampers nonlinearities, even

thought other sources of nonlinearities, as e.g. the landing gear system [16], are usually present and may be easily included using the same approach.

2 COMPUTING LIMIT CYCLES USING THE MULTIPLE INPUT DESCRIBING FUNCTION APPROACH

The Describing Function is based on the approximation of the nonlinear component under investigation by a sort of linear model, where a dependence is left on the amplitude of the input [5, 17]. This approach is usually denominated *quasi-linearization*. A quasi-linearized system is more difficult to handle than a linear one, nonetheless it retains the possibility of sharing some analysis methods typical of those systems, simplifying by far the analysis of nonlinear systems that otherwise must be based on direct time marching approaches, which may be very time-consuming, especially when hydraulic components are considered [20]. Moreover, the trends in system performance as functions of system parameters are more clearly displayed using the DF approach than with any other attack on nonlinear-system design.

The quasi-linearization is apt to reproduce the overall nonlinear response if the following *low-pass filter* hypothesis is valid: the linear part of the system must act as a low-pass filter with a pass band low enough to rule higher harmonics out of the response. This low-pass filtering hypothesis is usually verified but it is rarely possible to check it upfront, so the DF method is often considered an empiric approach.

To apply a DF method, let us consider an input for the nonlinear element $y(t) = f(u, \dot{u})$ of the type $u(t) = U\cos\omega t$. The output is expressible by means of the Fourier series expansion

$$y(t) = \sum_{i=0}^{\infty} |F_i(U,\omega)| \cos\left(i\omega t + \arg(F_i(U,\omega))\right) \quad (1)$$

where $F_i \in \mathbb{C}$ are the Fourier coefficients, and $\arg(\cdot) = \arctan\frac{\Im[\cdot]}{\Re[\cdot]}$. The DF is the complex fundamental-harmonic gain of a nonlinearity in the presence of a driving sinusoid, i.e.

$$\begin{aligned} N(U,\omega) &= \frac{F_1(U,\omega)}{U} \mathrm{e}^{j\arg(F_1(U,\omega))} \\ &= \frac{\Re[F_1(U,\omega)] + j\,\Im(F_1(U,\omega))}{U}. \end{aligned} \quad (2)$$

The nonlinear DF is the analogous of Transfer Function (TF) for linear elements, reducing identically to TF in case of purely linear elements. However, the coefficients are function of the input amplitude because they describe the output of a nonlinear element, and the linear superposition is not valid anymore.

Let us consider a generic linearized structural model expressed in second order form with lumped nonlinearities expressed by the force vector $\mathbf{F}$

$$\begin{aligned} &\mathbf{M}\ddot{\boldsymbol{q}} + \mathbf{C}\dot{\boldsymbol{q}} + \mathbf{K}\boldsymbol{q} = \mathbf{B}\mathbf{F} \\ &\mathbf{F} = \mathbf{F}\left(\boldsymbol{u}, \dot{\boldsymbol{u}}\right) \\ &\boldsymbol{u} = \boldsymbol{\Psi}\boldsymbol{q}, \end{aligned} \quad (3)$$

where $\boldsymbol{q}$ is an appropriate set of free generalized structural degrees of freedom associated to the shape functions $\boldsymbol{\Psi}$ which describe the displacement field $\boldsymbol{u}$ through a Ritz discretization.

To apply the DF approach, let us consider a single harmonic fed into the nonlinearity, i.e. $\boldsymbol{u} = \mathbf{U}\sin\omega t$. Then, by transforming the DF back in the time domain, Eq. (3) becomes

$$\begin{aligned} &\mathbf{M}\ddot{\boldsymbol{q}} + \mathbf{C}\dot{\boldsymbol{q}} + \mathbf{K}\boldsymbol{q} = \mathbf{B}\mathbf{F} \\ &\mathbf{F} = \Re[\mathbf{N}(\mathbf{U},\omega)]\boldsymbol{\Psi}\boldsymbol{q} + \frac{1}{\omega}\Im[\mathbf{N}(\mathbf{U},\omega)]\boldsymbol{\Psi}\dot{\boldsymbol{q}}, \end{aligned} \quad (4)$$

which can be rewritten as

$$\begin{aligned} \mathbf{M}\ddot{\boldsymbol{q}} + \left(\mathbf{C} - \frac{1}{\omega}\mathbf{B}\,\Im[\mathbf{N}(\mathbf{U},\omega)]\,\boldsymbol{\Psi}\right)\dot{\boldsymbol{q}} + \\ + \left(\mathbf{K} - \mathbf{B}\,\Re[\mathbf{N}(\mathbf{U},\omega)]\,\boldsymbol{\Psi}\right)\boldsymbol{q} = \mathbf{0}. \end{aligned} \quad (5)$$

The system is in a limit cycle condition if the unknown vector is equal to $\boldsymbol{q} = \mathbf{Q}_C \exp\left(j\omega_C t\right)$, i.e.

$$\begin{aligned} \left(-\omega_C^2\mathbf{M} + j\omega_C\mathbf{C}_N(\mathbf{Q}_C,\omega_C) + \right. \\ \left. + \mathbf{K}_N(\mathbf{Q}_C,\omega_C)\right)\mathbf{Q}_C = \mathbf{0}. \end{aligned} \quad (6)$$

with

$$\begin{aligned} \mathbf{C}_N &= \left(\mathbf{C} - \frac{1}{\omega_C}\mathbf{B}\,\Im[\mathbf{N}(\boldsymbol{\Psi}\mathbf{Q}_C,\omega_C)]\,\boldsymbol{\Psi}\right) \\ \mathbf{K}_N &= \left(\mathbf{K} - \mathbf{B}\,\Re[\mathbf{N}(\boldsymbol{\Psi}\mathbf{Q}_C,\omega_C)]\,\boldsymbol{\Psi}\right). \end{aligned}$$

The problem is similar to an eigenvalue problem. However, not all amplitude for the vector $\mathbf{Q}_C$ are valid since the DF elements buried in $\mathbf{C}_N$ and $\mathbf{K}_N$ depend on the amplitude itself. As a matter of fact, only the $\mathbf{Q}_C$ that solve the equation

$$\begin{aligned} \det\left(-\omega_C^2\mathbf{M} + j\omega_C\mathbf{C}_N(\mathbf{Q}_C,\omega_C) + \right. \\ \left. + \mathbf{K}_N(\mathbf{Q}_C,\omega_C)\right) = 0, \end{aligned} \quad (7)$$

is the correct one. So it is better to describe the vector $\mathbf{Q}_C = \alpha_C\mathbf{Q}_{\omega_C}$, where α_C is an amplitude

factor and $\mathbf{Q}_{\omega_C}$ is the eigenvector associated with the eigenvalue ω_C of Eq. (7). The Eq. (7) is a nonlinear complex equation with two real unknowns: the LCO frequency ω_C, and the amplitude α_C. Alternatively, the nonlinear problem can be formulated as

$$\begin{aligned}\left(-\omega_C^2\mathbf{M} + j\omega_C\mathbf{C}_N + \mathbf{K}_N\right)\mathbf{Q}_{\omega_C} &= \mathbf{0}\\ \mathbf{Q}_{\omega_C}^T\mathbf{Q}_{\omega_C} &= 1\end{aligned} \tag{8}$$

The result is $2(n+1)$ complex system of equations in the unknowns: $\mathbf{Q}_{\omega_C} \in \mathbb{C}^n$, α_C, ω_C, and can be solved using the classical Newton-Raphson approach.

2.1 Application to rotor ground resonance cases

The most basic model required to analyze ground resonance consists of four degrees of freedom (dofs) [2]: the two rotor cyclic lag modes plus the two in-plane hub displacement modes. However, when the real rotorcraft is analyzed, several additional degrees of freedom may be needed in order to correctly quantify the stability margins, as shown in [13]. To highlight the peculiarities of the DF approach the simple four dofs model is pursued here; however, no theoretical hurdles prevent the application of the same approach presented here to model with more degrees of freedom. Considering an hinged rotor of b blades mounted on a flexible support, it is possible to obtain the basic Ground Resonance system of equations by applying to the rotating parts a transformation of the rotating coordinates into multi-blade coordinates, describing the rotor motion in the inertial reference frame, as introduced by Coleman [1]:

$$\begin{aligned}Z_0 &= \frac{1}{b}\sum_{i=1}^{b}\zeta_i\\ Z_{nc} &= \frac{2}{b}\sum_{i=1}^{b}\zeta_i\cos n\psi_i\\ Z_{ns} &= \frac{2}{b}\sum_{i=1}^{b}\zeta_i\sin n\psi_i\\ Z_d &= \frac{1}{b}\sum_{i=1}^{b}\zeta_i(-1)^i.\end{aligned} \tag{9}$$

The last differential mode exist only if b is even. If the rotor is rotating at constant angular velocity Ω, then $\psi_i = \Omega t + i2\pi/b$. This transformation allows to switch from a periodic system of equations into a time invariant system of equations. It is useful to understand what happens when we try to apply this coordinate transformation to the nonlinear damper models. In this case on i-th blade is mounted a damper that delivers an output force when subject to a certain lag motion, i.e.

$$F_{di} = f_d\left(\zeta_i^0 + \zeta_i, \dot{\zeta}_i^0 + \dot{\zeta}_i\right) \tag{10}$$

where the terms $(\cdot)^0$ represent the reference lag motion of the blade around which the linearized model is set up. The single blade lag rotation can be obtained from the multi-blade coordinates applying the inverse of the transformation (9)

$$\zeta_i = Z_0 + \sum_{n=1}^{N}\left(Z_{nc}\cos n\psi_i + Z_{ns}\sin n\psi_i\right) + Z_d(-1)^i \tag{11}$$

where $N = (b-1)/2$ if b is odd, or $N = b/2 - 1$ if b is even. To apply the DF approach, let us consider a sinusoidal variation of the multi-blade coordinate vector $\mathbf{Z} = [Z_0, Z_{1c}, Z_{1s}, \ldots, Z_d]^T = \mathbf{Z}^C\mathrm{e}^{j\omega t}$.

$$\begin{aligned}\zeta_i = &\left(Z_0^C + Z_d^C(-1)^i\right)\mathrm{e}^{j\omega t} +\\ &+ \frac{1}{2}\sum_{n=1}^{N}\Big(\left(Z_{nc}^C + jZ_{ns}^C\right)\mathrm{e}^{j(\omega t - n\psi_i)} +\\ &+ \left(Z_{nc}^C - jZ_{ns}^C\right)\mathrm{e}^{j(\omega t + n\psi_i)}\Big).\end{aligned} \tag{12}$$

As a result, there are $2N+1$ harmonics fed into each damper

$$\begin{aligned}\zeta_i &= h_{i0}\,\mathrm{e}^{j\omega t} + \sum_{n=1}^{N}\left(h_{in}^{-}\mathrm{e}^{j(\omega - n\Omega)t} + h_{in}^{+}\mathrm{e}^{j(\omega + n\Omega)t}\right)\\ h_{i0} &= \left(Z_0^C + Z_r^C(-1)^i\right)\\ h_{in}^{-} &= \frac{1}{2}\left(Z_{nc}^C + jZ_{ns}^C\right)\mathrm{e}^{-jni2\pi/b}\\ h_{in}^{+} &= \frac{1}{2}\left(Z_{nc}^C - jZ_{ns}^C\right)\mathrm{e}^{jni2\pi/b}.\end{aligned} \tag{13}$$

So, in general for each blade $2N+1$ MIDF must be computed each one that depend on $4N+1$ parameters: the modules and the phases of the h coefficient of each harmonic expressed in Eq. (13). However, of all the b multi-blade dofs only the first two cyclic components are considered for stability analysis when linear models are considered since the other lag motions, either collective or reactionless, do not couple with hub motions. It must be verified if this hypothesis is still valid when nonlinear elements are considered.

The modules of the coefficients $h_{i1}^{\pm}$ are the same for every blade while the phase shift between the two harmonics depends from the blade position.

So, if the phase shift modified significantly the MIDF computed, a different quasi-linear model for each blade must be computed breaking the symmetry of the problem, and so the hypothesis of no intervention of the reactionless and collective modes. However, when the two frequency are not harmonically related and the nonlinearity is static the MIDF is independent from the phase shift (see [5]). For our cases this independence will be considered from here on, and it will be verified while computing the MIDF. Thus, the DF computed for each blade is the same and is equal to

$$\begin{aligned} F_{di} =& N^-(|h_1^-|,|h_1^+|,\omega,\Omega)h_{i1}^- \mathrm{e}^{j(\omega-\Omega)t} + \\ &+ N^+(|h_1^-|,|h_1^+|,\omega,\Omega)h_{i1}^+ \mathrm{e}^{j(\omega+\Omega)t}. \end{aligned} \tag{14}$$

All the forces of blade dampers must be summed up using the direct multi-blade transformation, Eq. (9), to compute the forces to be introduced in the inertial non-rotating reference frame. However, given the independence of the MIDF from the blade position that leads to Eq. (14), it is clear that the behavior is identical to that of a linear case (see [2]). The collective and the differential forces are null. For the cyclic cosine force component results

$$\begin{aligned} F_{1c} =& \frac{1}{2}\left(N^-\left(Z_{1c}^C + jZ_{1s}^C\right) + N^+\left(Z_{1c}^C - jZ_{1s}^C\right)\right)\mathrm{e}^{j\omega t} \\ F_{nc} =& 0 \qquad \forall n \neq 1, \end{aligned} \tag{15}$$

while for the cyclic sine force

$$\begin{aligned} F_{1s} =& \frac{j}{2}\left(-N^-\left(Z_{1c}^C + jZ_{1s}^C\right) + N^+\left(Z_{1c}^C - jZ_{1s}^C\right)\right)\mathrm{e}^{j\omega t} \\ F_{ns} =& 0 \qquad \forall n \neq 1. \end{aligned} \tag{16}$$

So, the forces output by the blade dampers excited by cyclic modes are composed only by cyclic components when approximated using the MIDF. Consequently the initial hypothesis of independence of the Ground Resonance problem from the collective and reactionless modes is still valid. In conclusion, the dampers' MIDF force in the inertial reference frame can be expressed as

$$\begin{aligned} \mathbf{F} =& \frac{1}{2}\begin{bmatrix} \Re[N^+ + N^-] & \Im[N^+ - N^-] \\ -\Im[N^+ - N^-] & \Re[N^+ + N^-] \end{bmatrix}\begin{Bmatrix} Z_{1c} \\ Z_{1s} \end{Bmatrix} + \\ &+ \frac{1}{2\omega}\begin{bmatrix} \Im[N^+ + N^-] & -\Re[N^+ - N^-] \\ \Re[N^+ - N^-] & \Im[N^+ + N^-] \end{bmatrix}\begin{Bmatrix} \dot{Z}_{1c} \\ \dot{Z}_{1s} \end{Bmatrix} \\ \mathbf{F} =& \mathbf{K}_{DF}\begin{Bmatrix} Z_{1c} \\ Z_{1s} \end{Bmatrix} + \mathbf{C}_{DF}\begin{Bmatrix} \dot{Z}_{1c} \\ \dot{Z}_{1s} \end{Bmatrix}. \end{aligned} \tag{17}$$

It is interesting to see what happens if it is considered the application of cyclic couples to the lead-lag dampers. This may happen if cyclic commands are applied to the rotor while the aircraft is on ground, or in general when an air resonance condition is considered. In this case two cyclic couples are applied around the lag hinge axis and must be reacted by the lead-lag dampers. The signal that is fed into the dampers can be represented as $\mathbf{Z} = [Z_{1c} Z_{1s}] = \mathbf{Z}^0 + \mathbf{Z}^C \mathrm{e}^{j\omega t}$.

$$\begin{aligned} \zeta_i &= h_{i1}^- \mathrm{e}^{j(\omega-\Omega)t} + h_{i1}^+ \mathrm{e}^{j(\omega+\Omega)t} + h_i^{\Omega-}\mathrm{e}^{-j\Omega t} + h_i^{\Omega+}\mathrm{e}^{j\Omega t} \\ h_i^{\Omega-} &= \frac{1}{2}\left(Z_{1c}^0 + jZ_{1s}^0\right)\mathrm{e}^{-jni2\pi/b} \\ h_i^{\Omega+} &= \frac{1}{2}\left(Z_{1c}^0 - jZ_{1s}^0\right)\mathrm{e}^{jni2\pi/b} \end{aligned} \tag{18}$$

In this case every MIDF will depend from the four amplitudes: $|h_{1n}^-|$, $|h_{1n}^+|$, $|h_i^{\Omega-}|$, $|h_i^{\Omega+}|$, plus the two frequencies ω, Ω. Also in this case the collective and the reactionless forces are null. For the cyclic forces an additional term must be considered

$$\mathbf{F} = \mathbf{K}_{DF}\begin{Bmatrix} Z_{1c} \\ Z_{1s} \end{Bmatrix} + \mathbf{C}_{DF}\begin{Bmatrix} \dot{Z}_{1c} \\ \dot{Z}_{1s} \end{Bmatrix} + \mathbf{K}_0\begin{Bmatrix} Z_{1c}^0 \\ Z_{1s}^0 \end{Bmatrix} \tag{19}$$

where

$$\mathbf{K}_0 = \begin{bmatrix} N^\Omega & 0 \\ 0 & jN^\Omega \end{bmatrix}. \tag{20}$$

In this case the nonlinear problem to be solved becomes

$$\begin{aligned} &\left(-\omega_C^2\mathbf{M} + j\omega_C\left(\mathbf{C} - \mathbf{B}\mathbf{C}_{DF}\mathbf{\Psi}\right)\right. \\ &\qquad \left. + \left(\mathbf{C} - \mathbf{B}\mathbf{C}_{DF}\mathbf{\Psi}\right)\right)\mathbf{Q}_{\omega_C} = \mathbf{0} \\ &\mathbf{Q}_{\omega_C}^T\mathbf{Q}_{\omega_C} = 1 \\ &\mathbf{K}_0\mathbf{Z}^0 = \mathbf{C}_e \end{aligned} \tag{21}$$

where $\mathbf{C}_e$ is the vector of cyclic couples applied to blade dampers.

2.2 Statistical linearization for computation of MIDF

A quasi-linear approximation for a nonlinear operator can be obtained by analyzing the operations performed by the nonlinearity on an input of specified form and approximating this operation by the *best* linear operation. The basic criterion used is the minimization of the mean squared difference between the output of the approximator and the output of the nonlinear operator [5].

Following this criterion it is possible to build, for a large class of typical nonlinear function, usually

static, several approximations like the Single Input sinusoidal Describing Function, the Dual Input DF where e bias term is considered or the Random Input DF. When dealing with nonlinearity with a more generic format, or when the form of the input signal is more complex, like the cases with several sinusoidal input considered here, the analytical approach may not be always feasible. In this case, it is better to proceed numerically relaying back to the basic criterion of minimization of the least square error.

Consider a generic nonlinear system where $y(t) = g(x, \dot{x})$. Given a certain input time history $x(t)$ with zero mean the nonlinear element has to be approximated by an equivalent linear element $y_e(t) = \beta_e \dot{x}(t) + k_e x + b$. The parameters of the approximation can be computed minimizing the expected value of the square of the error

$$\varepsilon = y - y_e = g(x, \dot{x}) - (\beta_e \dot{x}(t) + k_e x + b), \quad (22)$$

which means, for an ergodic process,

$$\min_{\beta_e, k_e, b} E\{\varepsilon^2\} = \min_{\beta_e, k_e, b} \lim_{T \to \infty} \frac{1}{T} \int_0^T \varepsilon^2(t) dt. \quad (23)$$

As a result the parameters of the best linearized model can be obtained (see [14])

$$\beta_e = \frac{E\{g(x, \dot{x})\dot{x}\}}{E\{\dot{x}^2\}} \quad (24)$$

$$k_e = \frac{E\{g(x, \dot{x})x\}}{E\{x^2\}} \quad (25)$$

$$b = E\{g(x, \dot{x})\}. \quad (26)$$

By running numerical simulation with the nonlinear component considered it is possible to evaluate the expectation when the system is trimmed, i.e. when all the internal states dynamics are damped out, and so compute numerically the different parameters for different type of input.

If a single sinusoidal input of frequency ω is considered, it is clear by comparing this results with Eq. (2) that

$$k_e \equiv \Re[N] \qquad \beta_e = \frac{\Im[N]}{w}. \quad (27)$$

In this case the process is exactly periodic of period $T_\omega = \frac{2\pi}{w}$. So, by choosing a final time equal to T_ω for the simulation the correct values for the parameters is computed. When multiple sinusoids are considered then

$$N_i = k_e + j w_i \beta_e. \quad (28)$$

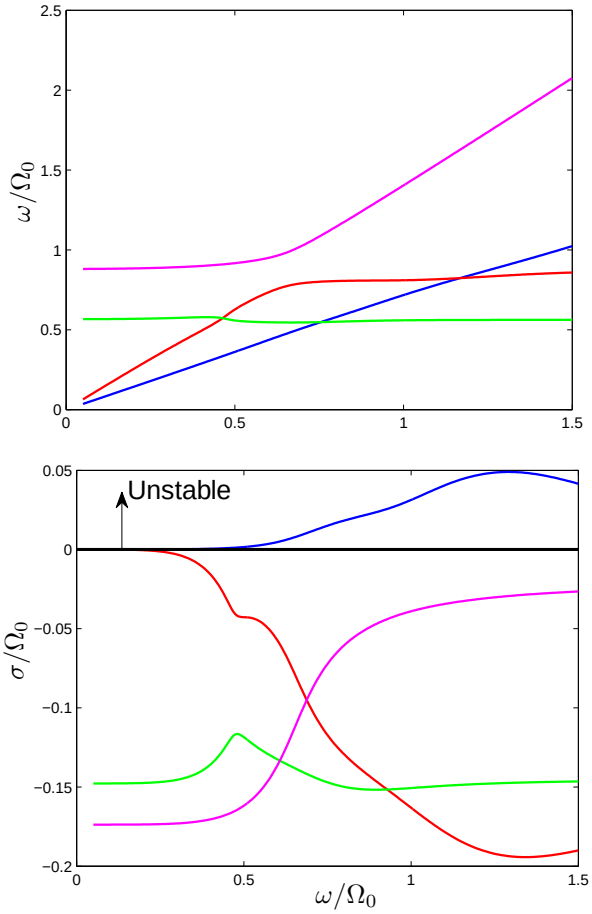

Figure 1: Evolution of the eigenvalues of Hammond's rotor eigenvalues for variable rotational speed with no lag dampers.

for this type of input, if the multiple frequencies considered are not harmonically related, the simulation *de facto* becomes a sort of Monte Carlo approach. By increasing the number of samples N the accuracy improves inversely to the square root of N [14].

3 Illustrative example Hammond's rotor

The very simple ground resonance example consisting of the single rotor helicopter suggested by Hammond in the classical paper [6] has been chosen from the open literature in order to present the potential of the synthesis approach proposed in the previous sections. In this case the simple four degrees of freedom model can adequately represent the phenomenon. Using the nominal model with parameters presented in Table 1, the rotor becomes significantly unstable from 50% RPM, see Figure 1.

Table 1: Hammond's rotor parameters

Nominal ang. velocity	Ω	200	rpm
Number of blades	b	4	
Lag hinge offset	e	0.3048	m
Blade mass	M_b	94.9	kg
Blade mass moment	S_b	289.1	kg m
Blade inertia moment	I_b	1084.7	kg m^2
Hub equiv. mass x	M_x	8026.6	kg
Hub equiv. mass y	M_y	3283.6	kg
Hub equiv. spring x, y	$K_{x,y}$	124.0e^4	N/m
Hub equiv. damping x	C_x	51079.	Ns/m
Hub equiv. damping y	C_y	25539.	Ns/m

Let us consider the case where hydraulic lead-lag dampers are used to suppress the ground resonance instability.

3.1 Hydraulic damper modeling

An hydraulic damper is composed by two chambers connected through an orifice. The basic dynamic equation of motions of these kind of systems are discussed in details in Ref. [12], and are here only briefly presented. First consider the classical mass conservation

$$\frac{d\rho V}{dt} = (\rho A\dot{u})_{in} - (\rho A\dot{u})_{out}, \tag{29}$$

where V is the volume of a chamber and A is the piston area. Considering that the density can be approximated by

$$\rho = \rho_0 \left(1 + \frac{1}{\beta}(p - p_0)\right), \tag{30}$$

so it results

$$\frac{dV}{dt} + \frac{V}{\beta}\frac{dp}{dt} = (A\dot{u})_{in} - (A\dot{u})_{out}. \tag{31}$$

The orifice flow occurs at high Reynolds number, so the behavior is essentially *turbulent*. In this case the volumetric flow rate is

$$Q = A_o C_d \sqrt{\frac{2|p_1 - p_2|}{\rho}}\,\mathrm{sign}(p_1 - p_2). \tag{32}$$

with A_0 the orifice area, and C_d the discharge coefficient. The volume of the chambers changes because the piston moves. So, by calling u the displacement of the piston, given the piston area A, the equations of the damper becomes

$$\dot{p}_1 = \frac{\beta}{V_0 - Au}\left(A\dot{u} - \lambda A_o C_d \sqrt{\frac{2|p_1 - p_2|}{\rho}}\right) \tag{33}$$

$$\dot{p}_2 = \frac{\beta}{V_0 + Au}\left(-A\dot{u} + \lambda A_o C_d \sqrt{\frac{2|p_1 - p_2|}{\rho}}\right), \tag{34}$$

with $\lambda = \mathrm{sign}(p_1 - p_2)$. The force developed on the piston is equal to

$$F = (p_1 - p_2)A. \tag{35}$$

Usually a Pressure Relief Valve (PRV) is added to the system. When the pressure difference $(p_1 - p_2)$ overcomes an assigned value Δp_0, the valve begins to open creating an additional orifice with an area that increase with the applied load, with a law that can be approximated usually as parabolic

$$A_{prv} = \alpha x + \gamma x^2. \tag{36}$$

If $|p_1 - p_2| > \Delta p_0$, the valve opening x results from the following differential equation

$$m\ddot{x} + c\dot{x} + kx = (|p_1 - p_2| - \Delta p_0) \tag{37}$$

where $k = K/A\ [F/L^3]$ is dimensionally a stiffness per unit area, and $m = M/A\ [M/L^2]$ is dimensionally a mass per unit area.

As a test case a model with the parameters presented in Table2 has been built here. The gear ratio τ is used to transform the blade lead-lag rotation into a linear translation of the damper's piston. It must be stressed that these numbers do not represent any real hydraulic damper but are only selected "in a reasonable manner" to build a numerical model useful to highlight the capabilities of the method.

4 RESULTS

4.1 Describing function of the hydraulic damper

It is possible to compute the MIDF using the hydraulic damper model described in the previous paragraph. For a single sinusoidal excitation the equivalent stiffness reaches it maximum before the saturation effect leads it again to lower values. Additionally, it is larger when the input frequency is high. This means that the maximum, as shown in Figure 2, is reached at small amplitude and $\omega \to 0$, since the effective input frequency is equal to $(\Omega - \omega) \to \Omega$.

Table 2: Hydraulic damper parameters

Piston Area	A	1.075e^{-3}	m^2
Piston stroke	d	0.187	m
Bulk modulus	β	1.53	GPa
$C_d\sqrt{2/\rho}$[a]		3.06e^{-2}	(m^3/kg)$^{\frac{1}{2}}$
Orifice section	A_0	9.8e^{-8}	m^2
PRV act. Press.	Δp_0	2.79	MPa
PRV stiffness	k	2e^4	N/m^3
PRV damping	c	5e^2	Ns/m^3
PRV mass	m	≈ 0	kg/m^2
PRV constant	α	2e^{-4}	
PRV constant	γ	5e^{-4}	
Gear ratio	τ	0.15	m/rad

[a] As suggested by [12]

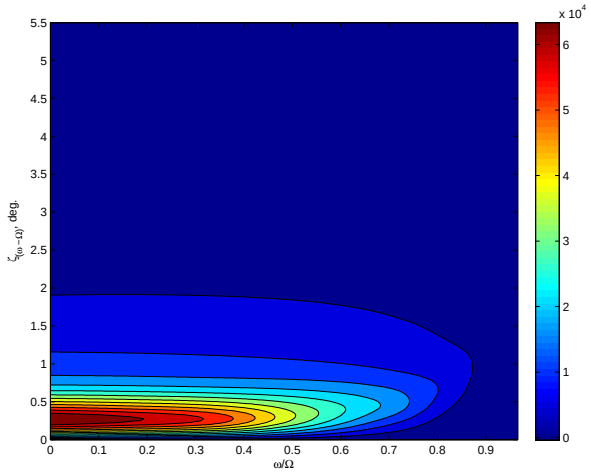

Figure 2: Equivalent stiffness in (N m/rad) of the hydraulic damper in the rotating frame at 100% RPM for different values of input frequency ω and amplitude h_1^-, with $h_1^+ = 0$.

The equivalent damping is maximum just before the saturation starts, while drops when the saturation is in place. Since the developed force depend essentially on the input velocity, the maximum is at low amplitudes at high input frequency and goes toward larger amplitudes when the input frequency drops. This behavior is shown in Figure 3.

The variation of the of equivalent damping and stiffness due to the inclusion of an additional harmonic at frequency $\omega + \Omega$ is quite sharp, see Figures 4 and 5.

4.2 LCO of the Hammond's rotor

The search of the LCO condition has been performed solving Eq. (8) using the classical

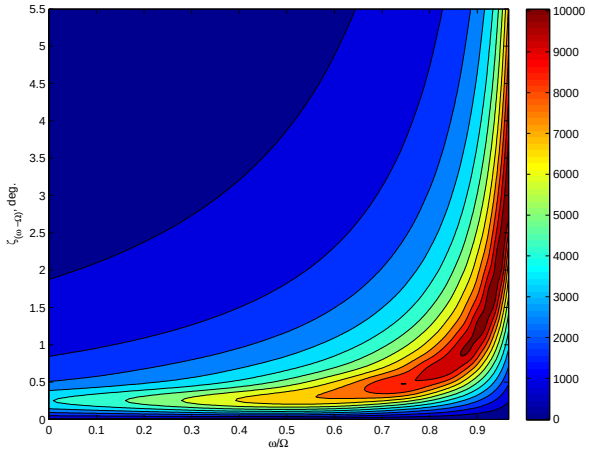

Figure 3: Equivalent damping in (N m s/rad) of the hydraulic damper in the rotating frame at 100% RPM for different values of input frequency ω and amplitude h_1^-, with $h_1^+ = 0$.

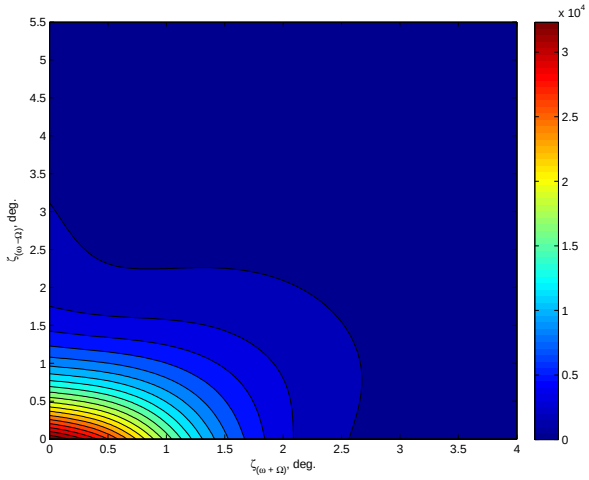

Figure 4: Equivalent stiffness in (N m/rad) of the hydraulic damper in the rotating frame at 100% RPM for different values of amplitudes h_1^-, and h_1^+ with $\omega = 0.75\Omega$.

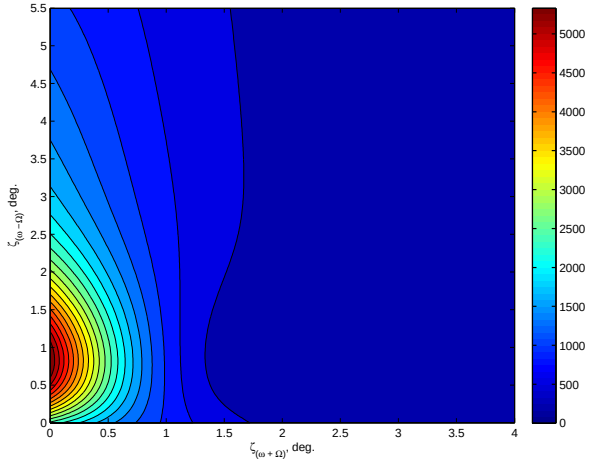

Figure 5: Equivalent damping in (N m s/rad) of the hydraulic damper in the rotating frame at 100% RPM for different values of amplitudes h_1^-, and h_1^+ with $\omega = 0.75\Omega$.

Levendberg-Marquardt algorithm applied to the problem formulated as nonlinear least-square [8]. The MIDF function are computed on a grid composed by 20 frequency points, 20 amplitude values for the low frequency mode, and 4 amplitude values for the high frequency mode. Then the values in the entire space are obtained using a cubic spline approximation.

Initially the amplitude of the signal at frequency $\Omega + \omega$ has been considered null. As a result a limit cycle at $\omega_C = 0.7195\Omega_0$ is obtained, with the amplitude shown in Table 3. The equivalent damping results equal to $\beta_e = 1436.3$ (N m s/rad), while the equivalent stiffness is $k_e = 1538.3$ (N m/rad). The resulting motion is characterized by a lateral oscillation that reaches the maximum acceleration of 0.365 g.

By considering also the second harmonic signal the equivalent values are modified only slightly, $\beta_e = 1434.3$ (N m s/rad) and $k_e = 1537.2$ (N m/rad). In fact, by running the solution in this case the same LCO is obtained, at the same frequency, and with a difference of ≈ 0.03 deg. in the blade lead-lag rotation amplitudes. So, the LCO behavior is essentially dominated by the the lower mode amplitude, as can be expected. To investigate the stability of the LCO it is possible to use the technique presented in [10]. If an exponentially shaped harmonic input is considered $\boldsymbol{q} = \mathbf{Q}\mathrm{e}^{\sigma t}\sin\omega t$ it is possible to use Eq. (8) to find the complex unknown $s = \sigma + j\omega$ and investigate the LCO stability. The system is stable if $d\sigma/d\alpha_c < 0$. To compute this derivative it is possible to use the derivative of

Table 3: LCO amplitude at 100% RPM.

Name	Real	Imag	unit
Z_{1c}	-2.3995	3.0360	deg.
Z_{1s}	-3.0797	2.4216	deg.
x	-0.0004	- 0.0088	m
y	-0.0014	- 0.0157	m
$\lvert h_1^- \rvert$	3.8937		deg.
$\lvert h_1^+ \rvert$	0.0245		deg.

equation (8):

$$\left(2s\frac{ds}{d\alpha_c}\mathbf{M} + \frac{ds}{d\alpha_c}\mathbf{C}_N + s\frac{dC_N}{d\alpha_c} + \frac{dK_N}{d\alpha_c}\right)\mathbf{Q} = \mathbf{0}. \tag{38}$$

To study the the stability of the LCO it is necessary to compute $d\sigma/d\alpha_c(s = j\omega_c) = \Re[ds/d\alpha_c]$. So

$$\frac{d\sigma}{d\alpha_c} = \Re\left[-\left(2j\omega_c\mathbf{M} + \mathbf{C}_N\right)^{-1}\left(j\omega_c\frac{dC_N}{d\alpha_c} + \frac{dK_N}{d\alpha_c}\right)\right]. \tag{39}$$

In this case the computation reveals that $d\sigma/d\alpha_c = 6.67$, which means that the LCO is an unstable one. as a result, it is possible to affirm that this unstable LCO is the separation orbit in state space between the basin of attraction of the stable orbit represent by the origin and unstable solutions. Consequently whenever the amplitude of this orbit is surpassed the system goes unstable.

4.3 LCO with cyclic couples applied

Consider a case where a $Z_c^0 = 0.3$ deg. cyclic 1/rev lead lag rotation is applied. In this case the equivalent damping and stiffness maps are significantly modified a shown by Figures 6 and 7.

In this case the resulting LCO has a frequency of $\omega_C = 0.72\Omega$, and the amplitude is shown in Table 4 and is slightly lower than the previous case. In fact due to the effect of the additional harmonics, the equivalent values are $\beta_e = 1441.7$ (N m s/rad) and $k_e = 1428.5$ (N m/rad), quite similar to the previous values at but at a lower amplitude.

The stability analysis also in this case reveals an unstable behavior similar to that of the previous solution.

5 Conclusions

The paper presented the application of the Multiple Input Describing Function approach to investigate the effect of nonlinear components on the ground resonance stability. It has been shown how

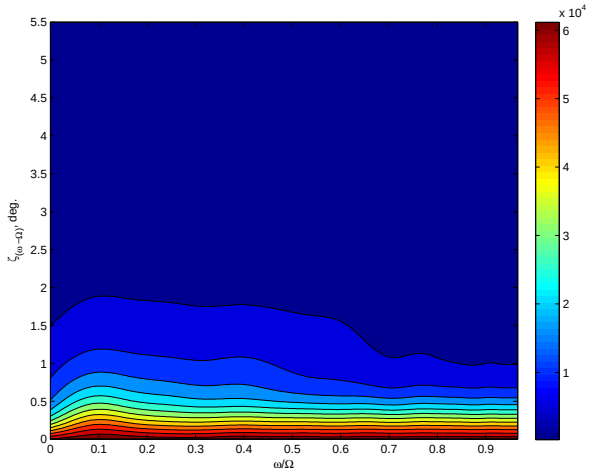

Figure 6: Equivalent stiffness in (N m/rad) of the hydraulic damper in the rotating frame at 100% RPM for different values of input frequency ω and amplitude h_1^-, with $h_1^+ = 0$ and Z_c^0 = 0.3 deg.

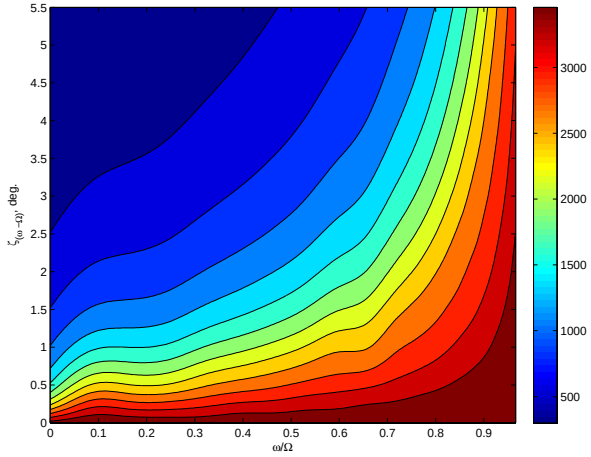

Figure 7: Equivalent damping in (N m s/rad) of the hydraulic damper in the rotating frame at 100% RPM for different values of input frequency ω and amplitude h_1^-, with $h_1^+ = 0$ and Z_c^0 = 0.3 deg.

Table 4: LCO amplitude at 100% RPM with Z_c^0 = 0.3 deg.

Name	Real	Imag	unit
Z_{1c}	3.5863	0.4727	deg.
Z_{1s}	0.4694	- 3.6320	deg.
x	- 0.0068	0.0046	m
y	- 0.0120	0.0087	m
$\|h_1^-\|$	3.6397		deg.
$\|h_1^+\|$	0.0229		deg.

a rigorous analysis must consider even in the simplest case more than one harmonics in input in the components that are mounted on the rotor. The MIDF are computed numerically using a simple simulation procedure. Several test have been performed to verify the capability of the the proposed approach. Several extension can be made considering for instance the effect of different levels of appropriately shaped noises injected as additional input into the nonlinear component to keep into account the effect of air turbulence. Multiple nonlinearities can be considered too, modeling in the same way also the another important component: the landing gear.

REFERENCES

[1] R. P. Coleman. Theory of self-excited mechanical oscillations of hinged rotor blades,. WR L-308, NACA, 1943.

[2] R. P. Coleman and A. M. Feingold. Theory of self-excited mechanical oscillations of helicopter rotors with hinged blades. REPORT 1351, NACA, 1958.

[3] R. Donham, S. Cardinale, and I. Sachs. Ground and air resonance characteristics of a soft in-plane rigid-rotor system. *Journal of the American Helicopter Society*, 14:33, 1969.

[4] F. Gandhi and I. Chopra. Analysis of bearingless main rotor aeroelasticity using an improved time domain nonlinear elastomeric damper model. *Journal of the American Helicopter Society*, 39:267–277, 1996.

[5] A. Gelb and W. E. Vander Velde. *Multiple-Input Describing Functions and Nonlinear System Design*. McGraw Hill Book Company, 1968.

[6] C. Hammond. An application of Floquet theory to prediction of mechanical instability. *Journal of the American Helicopter Society*, 19:14, 1974.

[7] M. Janowski and B. Tongue. Construction and analysis of a simplified non-linear ground resonance model. *Journal of Sound and Vibration*, 122(2):233–241, 1988.

[8] C. Kelley. *Iterative Methods for Linear and Nonlinear Equations*. SIAM, 1995.

[9] R. Lytwyn, W. Miao, and W. Woitsch. Airborne and ground resonance of hingeless ro-

tors. *Journal of the American Helicopter Society*, 16:2, 1971.

[10] M. Manetti, G. Quaranta, and P. Mantegazza. Numerical evaluation of limit cycles of aeroelastic systems. *Journal of Aircraft*, 46(5):1759–1769, 2009.

[11] P. Masarati, V. Muscarello, and G. Quaranta. Robust aeroservoelastic stability of helicopters: application to the air/ground resonance. In *AHS 67th Annual Forum*, Virginia Beach, VA, May 3–5 2011.

[12] H. E. Merritt. *Hydraulic Control Systems*. John Wiley & Sons, New York, 1967.

[13] V. Muscarello, P. Masarati, and G. Quaranta. An integrated environment for helicopter aeroservoelastic analysis: the ground resonance case. In *37th ERF*, Gallarate, VA, Italy, September 13–15 2011.

[14] J. Roberts and P. Spanos. *Random vibration and statistical linearization*. Wiley, Chichester, England, 1990.

[15] D. Tang and E. Dowell. Influence on nonlinear blade damping on helicopter ground resonance. *Journal of Aircraft*, 23:104–110, 1986.

[16] D. Tang and E. Dowell. Effects of non-linear damping in landing gear on helicopter limit cycle response in ground resonance. *Journal of the American Helicopter Society*, 1987.

[17] J. Taylor. *Wiley Encyclopedia of Electrical and Electronics Engineering*, chapter Describing Functions, pages 77–98. John Wiley & Sons, 1999.

[18] B. Tongue. Limit cycle oscillations of a non-linear rotorcraft model. *AIAA Journal*, 22:967–974, 1984.

[19] B. Tongue. Response of a rotorcraft with damping non-linearities. *Journal of Sound and Vibration*, 103:211–221, 1985.

[20] W. Welsh. Simulation and correlation of a helicopter air-oil strut dynamic response. In *43rd AHS Annual Forum*, pages 977–999, St Louis, Missouri, May 18–20 1987.

APPENDIX A: BASIC MATRICES FOR GROUND RESONANCE

The model is composed by two lead lag rotor modes and two support modes and the unknown vector is $\boldsymbol{q} = [Z_{1c}, Z_{1s}, x, y]^T$. The structural matrices, without considering the contribution of the lag dampers, are

$$\mathbf{M} = \begin{bmatrix} I_b & 0 & 0 & -\frac{b}{2}S_b \\ 0 & I_b & \frac{b}{2}S_b & 0 \\ 0 & S_b & M_x + bM_b & 0 \\ -S_b & 0 & 0 & M_y + bM_b \end{bmatrix}$$

$$\mathbf{C} = \begin{bmatrix} 0 & 2\Omega I_b & 0 & 0 \\ -2\Omega I_b & 0 & 0 & 0 \\ 0 & 0 & C_x & 0 \\ 0 & 0 & 0 & C_y \end{bmatrix}$$

$$\mathbf{K} = \begin{bmatrix} \Omega^2 I_b \left(\nu_b - 1\right) & 0 & 0 & 0 \\ 0 & \Omega^2 I_b \left(\nu_b - 1\right) & 0 & 0 \\ 0 & 0 & K_x & 0 \\ 0 & 0 & 0 & K_y \end{bmatrix}$$

$$\nu_b = \left(e\frac{S_b}{I_b}\right)$$

For the meaning of the symbols refer to Table 1. In this case the $\mathbf{\Psi}$ matrix is: $\mathbf{\Psi} = [\mathbf{I}\ \mathbf{0}]$, and the input matrix $\mathbf{B} = -\mathbf{\Psi}^T$.